AAS 12-214

A SURVEY OF SYMPLECTIC AND COLLOCATION INTEGRATION METHODS FOR ORBIT PROPAGATION

Brandon A. Jones[*] and Rodney L. Anderson[†]

Demands on numerical integration algorithms for astrodynamics applications continue to increase. Common methods, like explicit Runge-Kutta, meet the orbit propagation needs of most scenarios, but more specialized scenarios require new techniques to meet both computational efficiency and accuracy needs. This paper provides an extensive survey on the application of symplectic and collocation methods to astrodynamics. Both of these methods benefit from relatively recent theoretical developments, which improve their applicability to artificial satellite orbit propagation. This paper also details their implementation, with several tests demonstrating their advantages and disadvantages.

INTRODUCTION

Demands for orbit propagation capabilities continue to increase. For example, the US Air Force requires efficient and accurate propagation of a large number of space objects to assess the risks of satellite collisions. Additionally, numerical integrators commonly employed for orbital mechanics fail to meet stability requirements when propagating through reentry. These integration techniques also yield stability, accuracy, and computation issues when propagating for long periods of time, especially given that current research attempts to include effects in the coupling of the translational dynamics and rotational dynamics for long-term simulations.[1,2] Similarly, long-period integrations are required for certain interplanetary trajectory applications as well as planetary protection. These requirements stretch the limits of computational efficiency and accuracy, as well as extend the application of numerical propagation to new problems (e.g. low-thrust trajectories and propagation of probability density functions). Recent research focuses on techniques for reducing the evaluation time of the force model.[3–6] Instead, this paper considers the application of different integration methods for astrodynamics applications.

Common methods of orbit propagation rely on techniques largely developed over 30 years ago. The original Runge-Kutta methods date back to the turn of the 20th century.[7,8] These methods benefit from extensive research, with later developments allowing for the implementation of variational step sizes via embedded schemes and higher-order methods.[9–11] We note that all of these Runge-Kutta methods use an explicit formulation, since calculations using implicit methods were deemed too computationally intensive at the time. Current special perturbation propagation of the AF space object catalog relies on the Gauss-Jackson integrator first presented in 1924.[12,13] These classical techniques provide an excellent method for solving the initial value problem in traditional astrodynamics applications, but modern requirements demonstrate a need for updated methods.

Among the most recently developed integration techniques, the most promising appear to be those that are symplectic and/or use collocation. Pioneering works in symplectic integration first surfaced in 1956,[14] but began to mature with research published in the 1980s.[15,16] Unlike the previously mentioned classical

*Research Associate, Colorado Center for Astrodynamics Research, University of Colorado at Boulder, 431 UCB, Boulder, CO, 80309
†Member of Technical Staff, Jet Propulsion Laboratory, California Institute of Technology, 4800 Oak Grove Drive, M/S 301-121, Pasadena, CA 91109

methods, symplectic methods preserve the Hamiltonian, which should remain constant for conservative systems. Previous research demonstrates the use of these methods in celestial mechanics when using symplectic maps,[17–19] with more recent references providing more detailed treatments of numerical integration theory (see, e.g. Reference 20). Symplectic integrators tend to reduce integration error due to truncation, allowing for large time steps. Collocation methods also provide a potential method for trajectory propagation. Some implicit Runge-Kutta methods may also be characterized as a collocation method, and exhibit stability properties not available with the classic algorithms. With these stability characteristics, the same integrator may potentially be used for scenarios that require the integration through periods where the equations of motion transition between between non-stiff and stiff differential equations.

This paper summarizes several of these integration methods through the lens of artificial satellite propagation. This includes a combination of a literature survey of current and previous uses in astrodynamics, and presents several examples to demonstrate properties of these algorithms. The presentation of these algorithms includes implementation details allowing members of the astrodynamics community to easily implement these methods in their own software.

OVERVIEW OF HAMILTONIAN DYNAMICS

In this section, we present a basic overview of Hamiltonian dynamics, which serves as a basis for future discussion. We note that a more comprehensive discussion of the Hamiltonian forms of the governing equations of celestial mechanics may be found in, for example, Reference 21 or Reference 22. In general, the Hamiltonian H may be given by $H = H(\boldsymbol{p}, \boldsymbol{q}, t)$ where $\boldsymbol{q}$ is called the position vector and $\boldsymbol{p}$ is called the momentum vector. The differential equations are defined by

$$\begin{aligned} \frac{dp_i}{dt} &= -\frac{\partial H}{\partial q_i} \\ \frac{dq_i}{dt} &= +\frac{\partial H}{\partial p_i} \end{aligned} \tag{1}$$

where $i = 1...n$ and $\boldsymbol{p},\boldsymbol{q} \in \mathbb{R}^n$. Alternatively these equations may be written more compactly as

$$\begin{aligned} \boldsymbol{z} &= \begin{pmatrix} \boldsymbol{q} \\ \boldsymbol{p} \end{pmatrix} \\ \boldsymbol{J} &= \begin{pmatrix} \mathbf{0} & \boldsymbol{I} \\ -\boldsymbol{I} & \mathbf{0} \end{pmatrix} \\ \dot{\boldsymbol{z}} &= \boldsymbol{J}\nabla H \end{aligned} \tag{2}$$

where $\mathbf{0}$ and $\boldsymbol{I}$ are the $n \times n$ zero and identity matrices, respectively. $\boldsymbol{J}$ is the $2n \times 2n$ nonsingular, skew-symmetric structure matrix.

For two-body motion in Cartesian position and velocity coordinates $\boldsymbol{q}$ and $\boldsymbol{p}$, we may express the Hamiltonian in the separated form

$$H(\boldsymbol{q}, \boldsymbol{p}) = T(\boldsymbol{p}) + V(\boldsymbol{q}) \tag{3}$$

$$= \frac{\boldsymbol{p}^T\boldsymbol{p}}{2} - \frac{\mu}{|\boldsymbol{q}|}, \tag{4}$$

i.e. the sum of the kinetic and potential energies. We note that Eq. 4 is quadratic in the momentum variables, and, since H is independent of time, the system is *autonomous*. We note that most presentations of Hamiltonian mechanics employ notation based on such systems independent of time. However, formulations may easily be extended to *non-autonomous* systems.[20,23] When including temporal variations in H, e.g. $V = V(\boldsymbol{q}, t)$, Eq. 3 does not remain constant. Thus, we augment the equations with a new coordinate variable t. This yields the new system

$$
\begin{aligned}
\tilde{\boldsymbol{q}} &= \begin{pmatrix} \boldsymbol{q} \\ t \end{pmatrix} && (5) \\
\tilde{\boldsymbol{p}} &= \begin{pmatrix} \boldsymbol{p} \\ t \end{pmatrix} && (6) \\
\tilde{H}(\tilde{\boldsymbol{q}}, \tilde{\boldsymbol{p}}) &= H(\boldsymbol{q}, \boldsymbol{p}, t) + e && (7) \\
\dot{e} &= -\frac{\partial H(\boldsymbol{p}, \boldsymbol{q}, t)}{\partial t} && (8)
\end{aligned}
$$

where $\tilde{H}$ remains constant. Unless we wish to quantify the behavior of $\tilde{H}$ over time, we are not required to solve for e when generating a solution based on numerical techniques.

INITIAL VALUE PROBLEM

In its simplest form, a solution to the initial value problem (IVP) is a state y_{n+1} at some time t_{n+1} that results from the ordinary differential equation

$$\dot{y} = f(t, y). \tag{9}$$

and satisfies an initial condition

$$y(t_n) = y_n. \tag{10}$$

The function $f(t, y)$ is often referred to as the right-hand-side (RHS) function. When no analytic solution to Eq. 9 exists, which is true for all orbit propagation cases other than the two-body problem, numerical methods must be employed to generate an approximate solution. These numerical methods come in several forms, including: mapping, single-step, linear multistep, and extrapolation techniques. Sometimes, the distinctions between these methods weaken based on various implementations. This paper mainly considers single-step numerical integration methods with a limited treatment of multistep methods.

For the case where we seek to generate only a position solution, we may rewrite Eq. 9 as the second-order ODE

$$\ddot{y} = f(t, y, \dot{y}). \tag{11}$$

For these cases, a second-order integration method may be employed to directly solve for the position. Many cases in astrodynamics use a RHS form with no dependence on velocity, i.e. are separable. Example scenarios where the RHS function depends on velocity are: low-altitude orbits that include atmospheric drag, or the circular restricted three-body problem. Separable cases allow for some simplifications in the IVP solution method, which we discuss later.

Important Properties of Numerical Integrators

In this section, we discuss several properties of numerical integration techniques with various benefits to astrodynamics. We note that the more general subject of geometric integration encompasses both symmetric and symplectic methods, but both properties must not be satisfied to qualify as a geometric integration method.

Stability The stability of a numerical integration method refers to the dependence of error on integration step size h. For example, numerical integration of a system of stiff equations (e.g. satellite reentry) using a method with insufficient stability requires a step size smaller than the evolution of the dynamics. This effect results solely from the integrator and leads to inefficiencies in the propagation. For the system

$$f(y) = \lambda y, \qquad t \geq 0, \qquad y(0) = 1 \tag{12}$$

where $\lambda \in \mathbb{C}$ and $\mathrm{Re}(\lambda) < 0$, A-stability, sometimes referred to as linear stability, implies

$$\lim_{n\to\infty} y_n = 0, \qquad \forall\, h > 0. \tag{13}$$

Thus, for linear systems, step size selection only depends on desired accuracy.[24] However, we note that a lack of A-stability does not imply a solver is unsuited for all applications, but the property signifies an increased versatility of the given algorithm. L-stability[25] implies further improvements on the rate of decay for quickly decaying modes of the system, while B-stability[26] extends the A-stability criteria to nonlinear systems.

Symmetric A symmetric method preserves the time-reversibly properties of many dynamics problems. For two separate propagations $\phi_h : y_n \mapsto y_{n+1}$ and $\phi_{-h} : y_{n+1} \mapsto y_n'$, a non-symmetric method does not guarantee $y_n = y_n'$ (ignoring rounding error). Given the possible combination of backwards and forwards propagation in time for satellite propagation, a symmetric integrator allows for a more accurate propagation tool. This property of an integration method may often be determined through inspection, e.g. a symmetric distribution of Runge-Kutta nodes in a given time step.[20]

Symplectic A flow map $\boldsymbol{\phi}_{t,H} : \mathbb{R}^{2n} \to \mathbb{R}^{2n}$ of the Hamiltonian system H is symplectic if

$$\left[\boldsymbol{\phi}_{t,H}'\right]^T \boldsymbol{J} \boldsymbol{\phi}_{t,H}' = \boldsymbol{J}, \tag{14}$$

where $\boldsymbol{\phi}_{t,H}'$ signifies the Jacobian of the flow. Thus, the symplectic flow $\boldsymbol{\phi}_{t,H}$ preserves the Hamiltonian structure. Such methods, called symplectic integrators, preserve the first integral of the Hamiltonian system H, but at the possible expense of knowledge of the state at a specific instance in time. Thus, such methods yield a *qualitatively correct* description of the solution.[23] We provide an example that demonstrates this property later in the paper. References 20 and 23 provide a detailed explanation of these types of integrators and their relationship to the more general geometric integrators.

Overview of Common Integration Methods

In this section, we provide a brief overview of the two classes of integration methods most commonly employed in astrodynamics. These descriptions also set the stage for the introduction of the collocation and symplectic methods in the following sections. We note that comparisons between these common methods may already be found in the literature.[27–30]

Runge-Kutta (RK) Methods Independently developed by Carl Runge[7] and Wilhelm Kutta,[8] the ubiquitous Runge-Kutta (RK) methods provide a single-step method for solving the IVP. In a generalized form, an s-stage RK method may be written as

$$k_i = f\left(t_n + hc_i, y_n + h\sum_{j=1}^{s} a_{ij}k_j\right), \qquad i = 1, \ldots, s \tag{15}$$

$$y_{n+1} = y_n + h\sum_{j=1}^{s} b_j k_j. \tag{16}$$

The coefficients are often expressed in terms of the Butcher table

$$\begin{array}{c|c} c & A_{s\times s} \\ \hline & b^T \end{array}$$

where the integration (or Runge-Kutta) matrix A is comprised of the terms a_{ij}, and the vectors c and b include the c_i and b_j coefficients, respectively. RK methods are often classified by their order p and the number of stages s. Efficient methods minimize s for a given order p. When $a_{ij} = 0$ for $j \geq i$, this yields an explicit method in which each of the k_i terms may be determined sequentially. When this is not the case, i.e. we have an implicit Runge-Kutta (IRK) scheme, we use nonlinear solvers to generate k_i. The most common methods of RK-based orbit propagation use explicit schemes, which are easier to implement and benefit from decades of development. These methods fail to utilize the multi-core processing capabilities of modern computers for parallel evaluations of the RHS function. While concepts exist to define an explicit RK scheme that allows for the parallel computation of the s stages, such methods result in a reduced accuracy without increasing s.[31]

Embedded RK methods allow for autonomous determination of the step size based on maintaining a maximum local truncation error.[9–11] These methods add a minimal number of additional stages to generate a solution of higher (or lower) order. A comparison of these two solutions yields an estimate of the local truncation error, from which we may calculate the step size h. Such variable-step methods provide valuable computational savings for scenarios with large variations in the RHS function, and reduce the overall number of RHS evaluations.[28] The order of such methods is often written as $X(Y)$ where X is the order of the output solution and the Y-th order solution is used for step size control.

For this paper, we compare the collocation and symplectic methods (described later) to two embedded RK solvers: DOPRI 5(4)[10] and DOPRI 8(7).[11] The 7-stage DOPRI 5(4) method also serves as the integration scheme for MATLAB's `ode45()`.[32] For our tests, we use the DOPRI 5(4) solver provided in the CU-TurboProp propagation package.[33] All TurboProp integration routines utilize a common library of RHS functions, implemented in C, and include interfaces with both Python and MATLAB. Inspection of the DOPRI 5(4) integration scheme demonstrates that the extra k_7 used to generate the fourth-order solution equals k_0 for the next step. Thus, we use a first-same-as-last (FSAL) implementation to reduce the number of RHS evaluations to six per step. TurboProp currently provides a high-order solver in the form of the 13-stage RKF 7(8) algorithm.[9] However, this seventh-order method yields a larger truncation error when compared to the 13-stage DOPRI 8(7).[11,28] Hence, we add the DOPRI 8(7) integrator to TurboProp and use it as our eighth-order embedded solver. We note that FSAL may not be used with this method.

As we discuss below, this paper considers collocation methods in the form of IRK for orbit propagation. Such methods lend themselves to parallel implementation with good stability properties, but, like all parallel implementations, care must be taken to select the proper method for a given hardware configuration, i.e. the number of available processors.[31] When using fixed-point (or Picard) iteration over the interval h, each stage may be evaluated in parallel (see below). Other opportunities for parallelization exist. For example, previous research sought to leverage off of various properties of the integration matrix to perform evaluations of independent stages in parallel.[34,35] We do not provide any further discussion of these parallel methods in the current paper, but note their existence to encourage future consideration for astrodynamics applications.

Linear Multistep Methods Linear multistep methods use elements of polynomial interpolation and extrapolation to generate a new solution y_{n+1}. Unlike single-step tools, these methods use stored information from previous steps to form the new solution. This increases software complexity, both in storing previous steps and initialization of the algorithm, but multistep integrators typically provide faster propagation. Although we use the common eighth-order Gauss Jackson integrator (GJ 8) for the generation of high-fidelity truth orbits, we do not implement any recently developed linear multistep methods in the current paper. We note that efforts to date fail to generate a symplectic multistep integrator,[36–38] and any multistep methods of order greater than two cannot be A-stable.[39]

An alternative to the GJ 8 is the DIVA propagator.[40–45] It has been the primary integrator used at JPL for navigation and mission design applications since the 1960s, and it is currently implemented in JPL's next generation navigation and mission design software (MONTE/MASAR).[46] Comparisons to a variety of different algorithms have generally verified the utility of DIVA for the integration of trajectories for astrodynamics applications.[30,47,48] The algorithm itself uses a variable order, variable step size Adams method for solving ordinary differential equations that has been tailored specifically for integrating trajectories. More details about the algorithm may be found in Reference 49.

Description of Collocation Methods

A collocation method for approximating the solution to an ODE uses elements of polynomial interpolation where the first derivatives of the polynomial equal the slopes of the continuous solution $y(t)$ at a given set of nodes c_i. Given $c_i \in [0, 1]$ where $i = 1, \ldots, s$, a collocation polynomial solution satisfies

$$u(t_0) = y_0 \tag{17}$$

$$\dot{u}(t_0 + hc_i) = \dot{y}(t_0 + hc_i, u(t_0 + hc_i)) \tag{18}$$

with the solution to the collocation method $y_1 = u(t_0 + h)$. We note that the resulting polynomial $u(t)$ provides a *continuous* approximation of the system. Although several methods exist for using the collocation method to generate a solution to the IVP, all collocation methods may be expressed as an IRK method.[50] Additionally, we note that linear multistep methods represent a subset of collocation methods.

Collocation methods also benefit from a large body of research, which accelerated in the 1950s. Reference 51 discusses a different interpretation of the common implicit trapezoidal rule, which generates a solution based on the quadratic, shifted Legendre polynomial. These methods benefit from analytic definitions of the Butcher table for any number of stages s, with such definitions based on various quadrature rules. These schemes are commonly referred to as the Gauss-Legendre (GL) methods. A GL-IRK scheme using s stages yields a solution of order $p = 2s$.[52] This results in a minimal number of nodes required to achieve a solution of order p. Later characterization of these methods determined that they are symmetric,[20] A-stable,[53] B-stable,[26] *and* symplectic.[54] Unfortunately, such stability properties may be lost with implementation,[55] and, when compared to explicit symplectic integrators, the GL methods tend to be less computationally efficient.[20,56]

Other collocation methods exist, each with properties that make them more or less beneficial than the GL methods for some applications. The Radau IIA methods (see, e.g. Reference 20) include a stage at $c_s = 1$, thus incorporating information on the forces acting on the satellite at t_{n+1}. These methods provide a solution of order $p = 2s - 1$. The Radau IIA methods are A-, B-, and L-stable,[57] but are neither symplectic nor symmetric.[20] The Lobatto IIIA methods have stages at both of the end points, which allows for an FSAL implementation to reduce the number of RHS function evaluations. These methods are of order $p = 2s - 2$, A-, B-, and L-stable, but are not symplectic.

Although not prevalent at this time, application of collocation methods to orbit propagation and mission design exist. Previous boundary value problem applications of the Lobatto IIIA methods include trajectory optimization for Earth-Moon trajectories.[58,59] These same Lobatto IIIA methods were used for trajectory design for solar sail[60,61] and low-thrust trajectories[62,63] in the N-body problem for Lunar pole coverage.

Chebyshev collocation methods have also gained recent momentum in astrodynamics. Reference 64 demonstrated the application of such methods to fast and accurate orbit propagation, which included tests employing higher-degree gravity perturbations and atmospheric drag. These tests demonstrate more efficient propagation than DOPRI 8(7). We also mention that the formulation of Chebyshev collocation presented in Reference 64 allows for an adaptive order method. In Chapter 7 of Reference 65, the author provides a detailed treatment of collocation methods for orbit propagation. The reference includes orbital motion tests using polynomials defined by equally-spaced nodes, and a brief comparison with Chebyshev and Legendre collocation methods in simpler problems. Those results demonstrate that Legendre collocation outperforms Chebyshev collocation by about an order of magnitude in accuracy. However, these comparisons use polynomials of equal degree without compensating for the order of the resulting integration method. Recent research uses a method based on these Chebyshev methods, but does not require that Eq. 18 be strictly satisfied.[66]

In Figure 1, we illustrate the location of nodes c_i for three of the collocation methods mentioned. For these polynomials, we see an increase in concentration of c_i towards the endpoints of the time interval to prevent Runge's phenomenon. This results in oversampling, which reduces the overall efficiency of the integration method for high order schemes. An alternative method for orbit propagation reduces node density at the ends by using collocation with bandlimited functions.[67] This method sacrifices some accuracy for the sake of computation speed, symplecticity, and improved stability. The implementation of this method further reduces overall computation time through a combination of high-fidelity and low-fidelity RHS function evaluations in the iteration.

Gauss-Legendre Collocation Implementation

In this section, we describe the implementation of a GL-IRK method. We develop our GL method within the TurboProp framework, but note that MATLAB software designed for solutions expressed in a separated

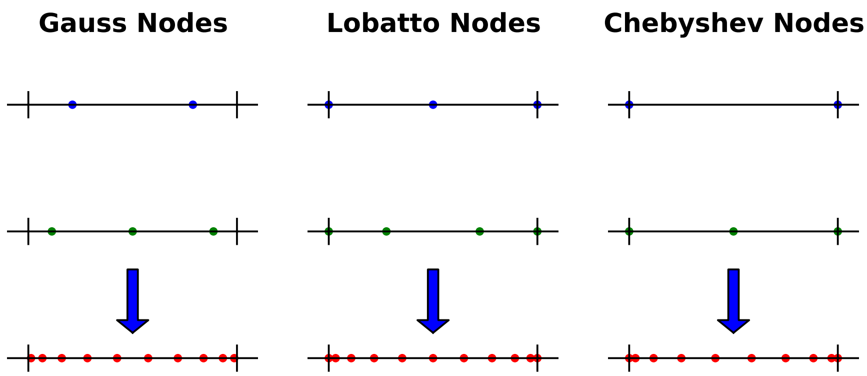

Figure 1. Example spacing of collocation nodes.

representation may be found online*. In the interest of brevity, we do not provide the Butcher tables for these methods. GL schemes for up to $s = 5$ may be found in the literature,[52] or generated via Mathematica for all $s^\dagger$. We also note that variable-step-size methods do exist when using the GL-IRK,[68,69] but are not described in this treatment.

The IRK methods require some form of iteration to solve the nonlinear system presented when solving Eq. 15. To reduce roundoff error when generating the k_i terms, we slightly change the formulation of the RK algorithm. Instead, we solve

$$\begin{aligned} Z_i &= h\sum_{j=1}^{s} a_{ij} f(t_n + hc_j, y_n + Z_j) && (19)\\ y_{n+1} &= y_n + \sum_{j=1}^{s} d_j Z_j, && (20) \end{aligned}$$

where

$$d^T = b^T A^{-1}, \tag{21}$$

i.e. we compute the smaller quantities Z_i in the nonlinear solver.[20,55,56] Eq. 20 prevents the s additional evaluations of the RHS after converging on the final solution for Z_j. Multiple techniques may be employed for the iterative process, with Reference 20 providing an overview and comparison of the most common tools based on fixed-point and Newton iteration. Although Newton iteration must be used to fully preserve stability properties when integrating stiff equations,[55] the additional computation time required tends to reduce their benefit for most situations.[20] Thus, we only consider fixed-point iteration in the present paper. We outline the method in Algorithm 1 for a scalar implementation, which may be easily altered for a vector $\boldsymbol{y}_n$.

Algorithm 1 Fixed-Point Iteration

while $\max\limits_{i=1,\ldots,s} (Z_i^k - Z_i^{k-1})/y_n > \delta$ and $k < k_m$ **do**
  for $i = 1, \ldots, s$ **do**
    $Z_i^{k+1} = h\sum_{j=1}^{s} a_{ij} f(t_n + hc_j, y_n + Z_j^k)$
  end for
  $k = k + 1$
end while

---

*http://www.unige.ch/∼hairer/software.html

†Command: `NDSolve`ImplicitRungeKuttaGaussCoefficients`[p, D], where D is the number of significant digits to display.

To reduce the number of iterations for the implicit solver, a good initial solution Z_i^0 must be generated. Several methods exist: extrapolation using the collocation polynomial,[20] additional evaluations of the RHS function using an embedded integration method,[70] equistage approximations,[71] or two-step, explicit methods.[72,73] Reference 20 compares the first three using Kepler's equation, and demonstrates that the embedded method yields a more accurate initial solution, and, thus, requires fewer iterations when used in the fixed-point algorithm. For the current implementation, we use the explicit integration method requiring three additional evaluations of the RHS. We note that this method requires the evaluation of $f(t_{n-1}, y_{n-1})$ and $f(t_n, y_n)$, thus FSAL-like methods may be employed to remove one evaluation per time step.

The initialization methods requiring additional function evaluations augment the IRK integration scheme with additional explicit stages to provide a relatively high-order approximation with a minimal impact to run time. We present the method requiring two additional function evaluations, which provides a prediction with accuracy of order $s+2$.[74] This yields the augmented Butcher table

$$\begin{array}{c|cccc}
0 & & & & \\
c & 0 & A_{s\times s} & & \\
1 & 0 & b^T & & \\
\eta & \eta_0 & \eta_{j=1,\dots,s} & \eta_{s+1} & \\
\hline
 & \nu_{i,0} & \beta_{s\times s} & \nu_{i,1} & \nu_{i,2}
\end{array}$$

where the new coefficients η_i, the matrices ν and β, and the stages of the previous integration step combine to form an embedded integration scheme to solve for the stages Z_i needed in the next step. We note that the j index in $\nu_{i,j}$ refers to the j-th column of the $s\times 3$ matrix, and this method also assumes a fixed h. Although the scheme is implicit, new evaluations of the RHS functions only require an explicit solution. Values for the integration schemes based on the GL methods with $s = 2, 3,$ and 4 may be found in Reference 74, with analytic methods for generating the table presented in the literature.[20] We provide the implementation details in Algorithm 2.

Algorithm 2 Iteration Initialization

if $t_n = t_0$ **then**
  $Z_i^0 = 0, \qquad i = 1, \dots, s$
else
  $Y_0 = y_{n-1}$
  $Y_j = y_{n-1} + Z_j \qquad j = 1, \dots, s$
  $Y_{s+1} = y_n$
  $Y_{s+2} = y_{n-1} + h \sum_{i=1}^{s+1} \eta_{2i} f(t_{n-1} + h\eta_i, Y_i)$
  $Z_i^0 = h \left(\sum_{j=1}^{s} (\beta_{ij} - b_j) f(t_{n-1} + hc_j, Y_j) + \nu_{i0} f(t_{n-1}, Y_0) + \sum_{j=1}^{2} \nu_{ij} f(t_{n-1} + h\eta_j, Y_j) \right)$
end if

Collocation methods provide a continuous solution to the IVP, which we may use to interpolate between time steps t_n. Although we may use interpolation methods specific to the collocation polynomial, we may instead compute a set of coefficients $\theta(t)$ for each output time that we use in

$$y(t) = y_n + h \sum_{j=1}^{s} \theta_j(t) f(t_n + hc_j, y_n + Z_j). \tag{22}$$

The coefficients $\theta_j(t)$ are generated by solving the Vandermonde-like system

$$\begin{bmatrix} 1 & 1 & \cdots & 1 \\ c_1 & c_2 & \cdots & c_s \\ \vdots & \vdots & \ddots & \vdots \\ c_1^{s-1} & c_2^{s-1} & \cdots & c_s^{s-1} \end{bmatrix}_{s\times s} \begin{bmatrix} \theta_1(t) \\ \theta_2(t) \\ \vdots \\ \theta_s(t) \end{bmatrix}_{s\times 1} = \begin{bmatrix} \tau \\ \tau^2/2 \\ \vdots \\ \tau^s/s \end{bmatrix}_{s\times 1} \tag{23}$$

with

$$\tau = \frac{t - t_n}{h}. \tag{24}$$

Assuming the Vandermonde matrix is non-singular (which is the case for the GL methods), we precompute its inverse to define a polynomial in τ. This yields a general method applicable to all collocation methods formulated as IRK. We note that such a method may be used for extrapolation ($|\tau| > 1$), which is also a common method used to initialize the iteration procedure in the next time step. Such methods are often employed in variable-step IRK solvers.[55]

Description of Symplectic Methods

Symplectic solutions of the IVP provide a numerical method for performing a canonical transformation of a given dynamical system. These methods preserve the Hamiltonian flow, i.e., the first integral of the equations of motion. However, the algorithms tend to be more coupled with the underlying Hamiltonian equations of the given system. We do not seek to provide a full survey of symplectic methods since several may already be found in the literature[75–78] Here, we describe some previous applications of these methods to orbital motion. We note that symplectic integration methods for rigid body dynamics exist,[20,23,79–81] but do not provide any details on these equally useful applications

Symplectic integration methods already have a history of use in celestial mechanics. The most prominent application of these techniques demonstrates the long-term, chaotic evolution of the solar system for up to 1 billion years.[19,82] Researchers used similar methods to study the evolution of the distribution of Kuiper belt objects.[83] Another example application includes analysis of the long-term behavior of short-period comets.[84] These previously mentioned techniques use low-order methods and assume the dynamics may be separated into

$$H = H_{\text{kep}} + H_{\text{pert}} \tag{25}$$

where H_{kep} represents the Hamiltonian defined by Keplerian motion, and H_{pert} represents the Hamiltonian due to small perturbations, e.g. third-body effects. Upon this separation, low-order integrators specific to the given problem may be developed. Higher-order methods have also been suggested and evaluated for celestial mechanics,[85–87] each with relative advantages and disadvantages. These applications imply a possible use for Earth-based scenarios.

Early comparisons of symplectic integrators with previously existing methods described their advantages for many long-term scenarios, but mention a strong disadvantage in terms of the lack of step size adaptation. For celestial mechanics, a lack of variable-step capabilities creates inefficiencies when propagating a system with close encounters and large eccentricities.[88–91] Early tests of symplectic integrators demonstrate that classical methods of step size control fail to preserve the Hamiltonian flow.[88,92,93] Attempted solutions employed time step selection techniques based on ad hoc methods specific to a given problem.[90,91] More recently, general methods were developed to provide variable-step capabilities in geometric integrators. Other techniques, based on a Sundman transformation, used a fixed step in a fictitious time and a scenario-specific transformation function to create an adaptive time step method.[94–98] Such a transformation provides a symmetric method, but, in general, is no longer symplectic.[23] However, when combined with a Poincaré transformation, the symplectic flow may be preserved and the methods meet the necessary requirements for adaptability in Hamiltonian systems.[69,99,100]

Other recent studies seek to characterize and develop symplectic integration techniques more applicable to Earth-based simulation of artificial satellites. The early tools developed for celestial mechanics make two primary assumptions: (1) H_{pert} is small compared to Keplerian motion, and (2) all forces are conservative. This raises the question: How suited are these methods to the more dynamic, non-conservative environment of low-earth orbit? Assuming the proper formulation of the system, symplectic integration methods demonstrate desired accuracy when gravity perturbations are included.[101,102] Although the Hamiltonian typically describes a conservative system, dissipative terms may be added to formulate a system with non-conservative forces, e.g. drag. Methods for including non-conservative forces in the Hamiltonian formulations, with the caveat that such dissipative effects are relatively small, have been presented in the literature.[20,102–105] We note that such forces cause a change in H over time, which will be exhibited in the resulting integration. Including such forces in a symplectic integrator generates a trajectory with dissipation representative of the true dynamics of the system. Although some studies exist demonstrating the use of symplectic integrators for Earth-centric orbits,[106,107] more research is required before they may be adopted for qualitative studies of artificial satellites.

Störmer-Verlet Composition Implementation

We now describe the implementation of a symplectic integrator based on a combination of the Störmer-Verlet scheme and a composition of symplectic maps. We note than MATLAB versions of this algorithm may also be found online*, but we use a version in C written for TurboProp.

Upon expressing the dynamical system in Hamiltonian form using canonical coordinates $\boldsymbol{q}$ and $\boldsymbol{p}$ and assuming that H is quadratic in $\boldsymbol{p}$, the Störmer-Verlet scheme may be written as

$$\boldsymbol{q}_{n+1/2} = \boldsymbol{q}_n + \frac{h}{2}\boldsymbol{p}_n \tag{26}$$

$$\boldsymbol{p}_{n+1} = \boldsymbol{p}_n - h\nabla_{\boldsymbol{q}} H(\boldsymbol{q}_{n+1/2}) \tag{27}$$

$$\boldsymbol{q}_{n+1} = \boldsymbol{q}_{n+1/2} + \frac{h}{2}\boldsymbol{p}_{n+1}. \tag{28}$$

This method is explicit, symmetric, symplectic, and second order.[20] For a Hamiltonian not quadratic in $\boldsymbol{p}$, we substitute $\nabla_p H(\boldsymbol{p}_j, \boldsymbol{q}_{n+1/2})$ for $\boldsymbol{p}_j$ in Eqs. 26 and 28, but the resulting scheme may be implicit. We note that, if $\boldsymbol{q}_{n+1}$ is not required, then Eqs. 26 and 28 may be replaced with

$$\boldsymbol{q}_{n+1/2} = \boldsymbol{q}_{n-1/2} + h\boldsymbol{p}_n. \tag{29}$$

We use this later form during propagation when q_n is not output or for an intermediate stage in the composition method described below.

Composition methods use a collection of substeps based on a low-order symplectic map to generate a high-order method. Like all splitting methods, such techniques reduce the differential equation into a collection of simpler equations to integrate. The composition of these solutions then yields the solution of the total system. An extensive survey of these splitting methods may be found in Reference 108. If the system Hamiltonian may be expressed in a separated form similar to Eq. 3, then a composition of symplectic flows is also a symplectic flow.[23] High-order methods may then be developed using s-fold compositions

$$\Phi_{h,H} = \phi_{w_s h,H} \circ \phi_{w_{s-1} h,H} \circ \cdots \circ \phi_{w_2 h,H} \circ \phi_{w_1 h,H}, \tag{30}$$

where $\sum w_i = 1$ and $\phi_{\Delta t}$ is a second-order, symmetric, and symplectic method, e.g., the Störmer-Verlet scheme.[85] Assuming a proper selection of $\{w_i\}$, it may be demonstrated that such compositions of a low-order method generate a high-order approximation.[108] Thus, high-order integration only requires a Störmer-Verlet solver and the composition scheme $\{w_i\}$ to create a high-order symplectic integrator. In terms of implementation, we simply chain together evaluations of the Störmer-Verlet scheme, each with step size $w_i h$. A table of example schemes may be found in Reference 23. Here, we use the eighth-order, 17 stage method of Reference 109, which we refer to as SVC 8.

To minimize round-off error, and the loss of symplecticity due to numerical error, we must employ compensated summation[20,110,111] in the Störmer-Verlet scheme. This method, presented in Algorithm 3, preserves digits normally lost with the addition operation in Eqs. 26-29. We note that some aggresive compiler optimizers, e.g. the Intel C/C++ compiler, use associative properties to improve computation speed at a slight cost to precision. When this is the case, it removes the benefits of compensated summation. However, such optimizations can be disabled†.

*http://www.unige.ch/∼hairer/software.html

†Use compile-time options for Intel C/C++ compiler: `-fp-model precise -fp-model source`

Algorithm 3 Compensated Summation

Require: y_0, $\{\delta_n\}$, and $\epsilon = 0$
  for $n = 0, \ldots, n_m$ **do**
    $\alpha = y_n$
    $\epsilon = \epsilon + \delta_n$
    $y_{n+1} = \alpha + \epsilon$
    $\epsilon = \epsilon + (\alpha - y_{n+1})$
  end for

DEMONSTRATION OF METHODS

In this section, we demonstrate some of the capabilities of the GL and composition methods. For these cases, we use two principle orbits: (1) a nearly-circular low-Earth orbit (LEO), and (2) a Molniya orbit. The LEO case has an initial semimajor axis altitude of 300 km, and eccentricity of 10^{-4}, and an inclination of 45 deg. The Molniya case has a semimajor axis of 26,562 km, an eccentricity of 0.741, and an inclination of 63.4 deg. The eccentricity vector for both cases lies in the inertial X-Z plane in the positive X direction, and the satellites initially start at periapsis.

Baseline

In this section, we present results from several baseline tests used to illustrate the relative performance of the classical integration methods employed in future sections. For this test, we duplicate tests previously used in the literature,[28] and extend the test to a higher-fidelity propagation using the test orbits previously described.

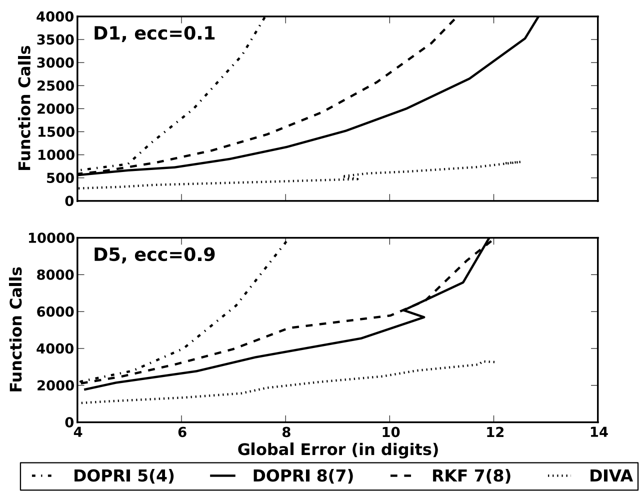

Figure 2. Work-Precision Plots Duplicating the Tests from Reference 28

References 28 and 30 compare many of the Runge-Kutta and linear multistep methods commonly used in orbit propagation. In Figure 2, we duplicate the D1 and D5 tests described in Reference 28, but instead use the DOPRI 9(7), DOPRI 5(4), RKF 7(8) and DIVA propagators available for this paper. We note that the D1 and D5 tests simulate two-body orbits with an eccentricity of 0.1 and 0.9, respectively. Initial conditions use normalized coordinate systems, and quantify precision by the global integration error, i.e. the error at the final time. These orbits are propagated for 20 time units, or approximately 3 orbit periods. The results for the D1 case match those presented in Reference 28 to within variations due to the selected time step determination algorithm. As expected, the multistep, variable-order, variable-stepsize DIVA propagator outperforms the embedded RK methods.

The tests of References 28 and 30 use the two-body problem for various eccentricities with truth defined by Kepler's equation. For the current paper, we include some tests using higher fidelity dynamics and the DOPRI 8(7), DOPRI 5(4), and GJ 8 methods. Unfortunately, making the necessary changes to DIVA to ensure the use of equivalent force models was not feasible in time for this comparison.

For the higher-fidelity tests, we add the most commonly used special perturbations to the force model. We use the GGM02C[112] model up to degree 70 for gravity perturbations, an exponential atmospheric density model,[113] Moon and Sun third-body perturbations with ephemerides determined using the 2006 Astronomical Almanac approximation,[114] and a constant area-to-mass ratio of 0.01 m^2/kg. We generate results using both the LEO and Molniya cases. We propagate these orbits for two days in all three of the methods mentioned previously, with states output every 100 s. We use a GJ 8 propagation with a step size of one second as the reference solution, which we chose since previous studies demonstrate the improved accuracy of multistep methods compared to explicit Runge-Kutta.[28] For the fixed-step methods, we vary the step size h to achieve a given accuracy, and vary the relative tolerance in the variable-step integrators to achieve similar accuracy.

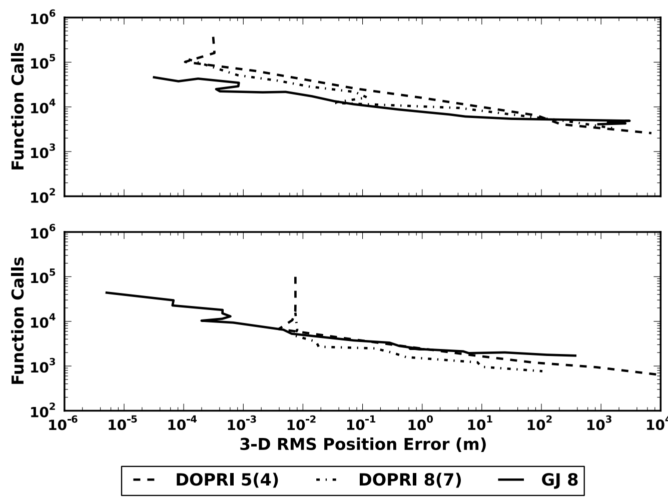

Figure 3. Work-Precision Plots for the Embedded RK Methods for the LEO (top) and Molniya (bottom) cases.

Figure 3 provides the work-precision diagram for the three integration methods. For the LEO case, the GJ 8 performs better than the RK methods, which is expected. In the Molniya case, the oversampling at apoapsis for the GJ 8 propagator increases the work required for the propagation. The maximum precision exhibited by the RK methods matches the limit exhibited in previous studies for the two-body tests.[28]

Collocation Capabilities

In this section, we profile the performance of the GL-IRK methods in comparison with the explicit RK methods. We consider GL methods of fourth, sixth, and eighth order, and again use the GJ 8, one-second solution as the reference. As mentioned previously, we may use a parallel implementation of the RHS function evaluations when iterating. Thus, we compare both the number of RHS evaluations and the total computation time required for the two-day propagation.

When comparing software runtimes, it is important to define the hardware and software tools used. Except for the GJ 8 integrator, all of these tools are implemented in the TurboProp framework based on the C language. We use the Intel C/C++ compiler with `-O3` optimization. We note that we disable optimization

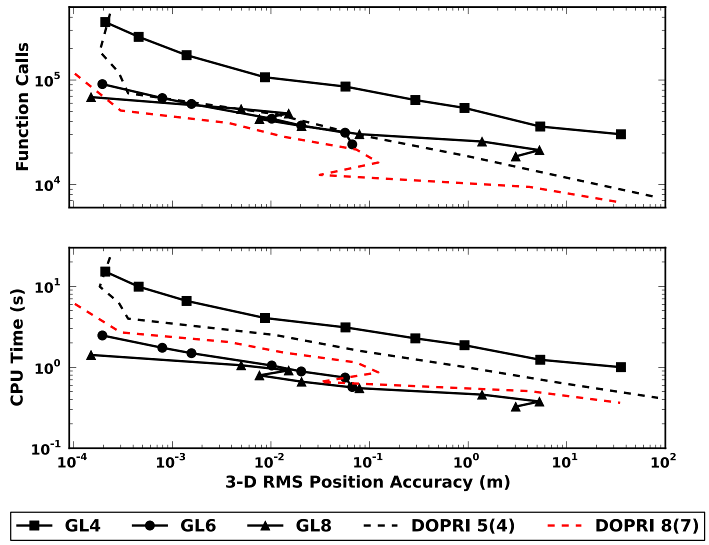

Figure 4. LEO Work-Precision and Execution Time-Precision Plots for the Collocation Methods

based on associative properties (see discussion of compensated summation). The GJ 8 software available for this study was implemented in Fortran 90/95 with the Intel ifort compiler. Given the difference in languages and compilers, we do not compare the GJ 8 runtimes to the other routines. We run these tests on a dedicated system running RedHat Enterprise 5 Linux on a Dual Intel quad-core 2 GHz processor, which allows up to eight parallel processes.

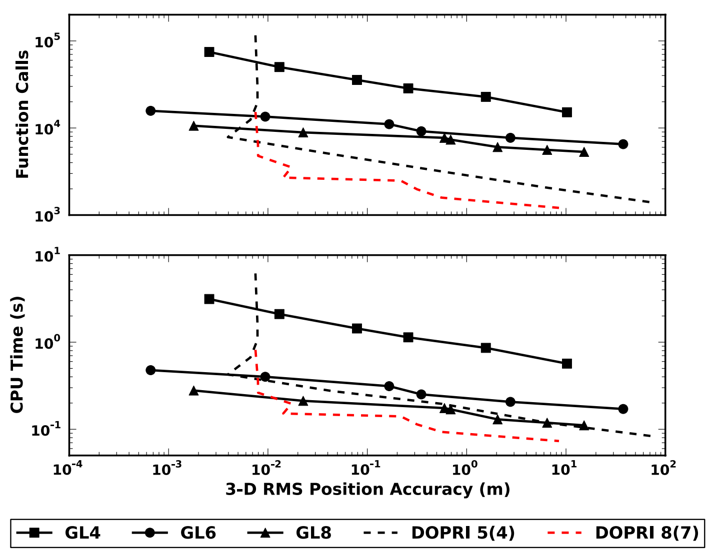

Figure 5. Molniya Work-Precision and Execution Time-Precision Plots for the Collocation Methods

Figure 4 compares the GL methods to the embedded Runge-Kutta methods for the LEO orbit. In terms of function calls, the iteration results in more RHS evaluations than the embedded methods. However, we see a computation time reduction with the parallel, higher-order GL-IRK methods. In fact, we see that a sixth-order GL-IRK outperforms the eighth-order DOPRI 8(7).

We provide results for the Molniya case in Figure 5. The highly-eccentric orbit reduces the efficiency of the fixed-step methods, thus yielding results where the embedded techniques require less computation time and RHS evaluations. For a more valid comparison, we must implement a variable-step implementation of the IRK methods,[68,69] which we plan to pursue for future tests.

Symplectic Capabilities

To demonstrate the capabilities of symplectic integration, we perform a 25-year propagation of a 300 km altitude, nearly circular orbit about the Earth. For this case, we use the LEO test case. We perform this test with both the SVC 8 and DOPRI 8(7) methods. For the DOPRI 8(7) algorithm, we use a relative tolerance of 10^{-15}, and select a time step of 500 s for the SVC 8 method. We compare the results to the true results of Kepler's equation.

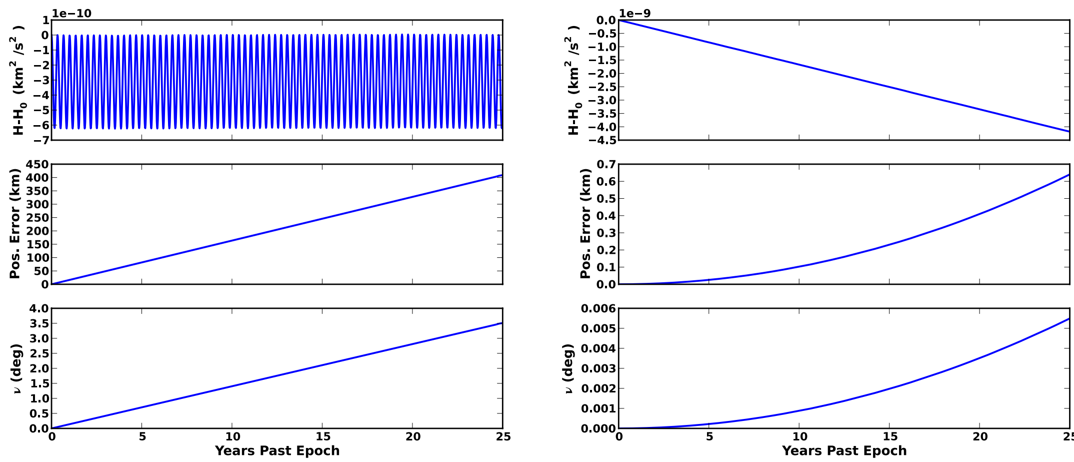

(a) SVC 8, Exec Time: 1.33 s

(b) DOPRI 8(7), Exec Time: 23.5 s

Figure 6. Features of a 25-Year Propagation of a LEO Satellite

In Figure 6, we provide some of the key features of the propagations, including the change in the Hamiltonian H, the root-sum-square position error, and the error in true anomaly ν of the orbit for both integrators. We see that the Hamiltonian oscillates for the SVC 8 case, but such variations are uniformly bounded with an amplitude less than the change in H in the DOPRI 8(7) results. The execution time required for the integration is also 17.7 times faster than the DOPRI 8(7) execution time. However, we see the accuracy of the SVC 8 method degrades over time. The propagator exhibits a linear growth in phase error, which we see in the value of true anomaly. Although we do not provide a plot, execution of the SVC 8 method with a step size of 50 s yields a global error of 0.18 m and an execution time of 15.9 s. The oscillations of the Hamiltonian for this last case are nearly zero. Thus, for a sufficiently small step size, the SVC 8 method performance exceeds that of DOPRI 8(7) for both accuracy and run time.

In Fig 7, we plot the $h = 500$ s SVC 8 solution in phase space, along with the truth defined by Kepler's equation. For this plot, we only include the SVC 8 solution for every 115.75 days. The plot demonstrates that the symplectic integrator preserves the phase space structure, i.e., area, over the full 25 year span. As indicated by the error in true anomaly in Figure 6(a), position error results from a difference in the phase. This result is commensurate with the analysis of Reference 115, which determined that a phase offset occurs as a function of the number of steps per period.

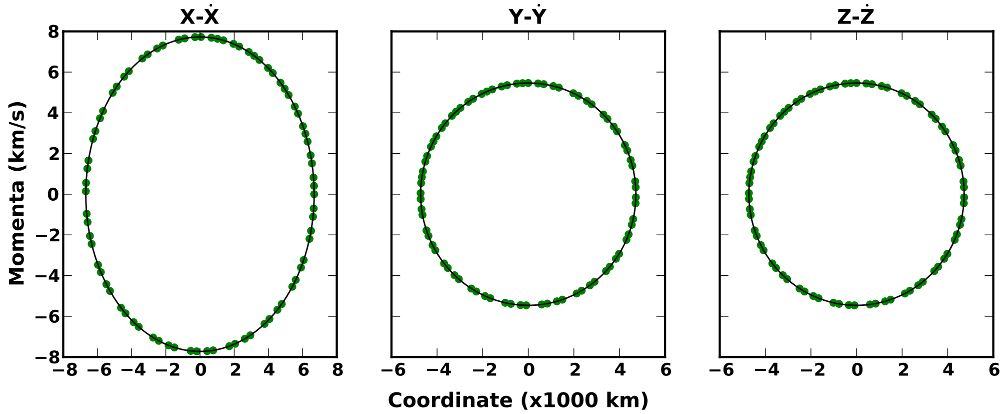

Figure 7. Phase Space Plots of SVC-8-Determined State (green dots) and Truth (black line)

PROSPECTS

In this paper, we summarized some applications of collocation and symplectic methods to astrodynamics. This included a description of applicable developments in these integration techniques and a survey of their application in astrodynamics. This paper represents the results of initial efforts to provide a comprehensive survey of the application of new integration techniques to astrodynamics, with a final goal of identifying possible applications for the propagation of artificial satellites both for Earth orbit and interplanetary trajectories. Based on the current maturity of their applications to orbit propagation and mission design, collocation methods may immediately be applied to rapid orbit propagation. However, some work is still required to further classify which methods best meet the requirements of astrodynamics, e.g. the largest reduction in computation time, use for propagating through re-entry, etc. Symplectic methods still require further development, although initial efforts demonstrate potential for their application.

This paper also described key features for the implementation and application of implicit Runge-Kutta and symplectic integrators. We presented elements required for the implementation of the Gauss-Legendre collocation methods, specifically the algorithms required for developing software that uses the implicit Runge-Kutta definition of these methods. For the symplectic integrators, we described the implementation of the second-order Störmer-Verlet method, and a high-order propagation method using the composition of the lower-order method. Examples demonstrate the reduced computation time found with a parallel implementation of the Guass-Legendre methods, with results motivating future exploration of such implicit techniques already developed for parallel computation. The higher-order, symplectic propagation test demonstrated the qualitative benefits of such methods for long-term propagation, albeit at the expense of accuracy at a discrete point in time. Such methods may be used for certain types of analyses, e.g. estimating the change in general properties of an orbit over very long time spans.

ACKNOWLEDGMENTS

Brandon Jones's portion of this research was partially funded by the Air Force Research Laboratories. Rodney Anderson's contribution to this research has been carried out at the Jet Propulsion Laboratory, California Institute of Technology, under a contract with the National Aeronautics and Space Administration. The authors would also like to thank Juan Arrieta-Camacho, Ahlam Amy Attiyah, Todd Ely, and Dan Grebow for their comments and suggestions on the manuscript.

NOTATION

A	matrix of $a_{i,j}$ coefficients, often called the Runge-Kutta integration matrix
$a_{i,j}, b_j, c_i$	Runge-Kutta integration scheme

d_j	scaled Runge-Kutta scheme coefficients
e	time momenta
$f(t, y)$	ordinary differential equation function
H	Hamiltonian
h	step size
$\boldsymbol{I}$	Identity matrix
i, j, n, k	dummy indices
k_i, Z_i	intermediate Runge-Kutta stage variables
$\boldsymbol{J}$	Hamiltonian structure matrix
$\boldsymbol{p}, p_i$	canonical momenta
$\boldsymbol{q}, q_i$	canonical coordinates
s	number of Runge-Kutta stages
$T(\boldsymbol{p})$	Kinetic energy
t	time
$u(t)$	collocation polynomial
$V(\boldsymbol{q})$	Potential energy
y, Y	state variable
$\boldsymbol{z}$	canonical state vector
α	stored value
δ	change in variable
ϵ	summation compensation term
η, ν, β	iteration initialization integration scheme matrices
$\theta(t)$	collocation interpolation coefficient
λ	scale parameter
μ	gravitation parameter
$\phi_{h,H}, \Phi_{h,H}$	flow maps
τ	scaled time

REFERENCES

[1] D. J. Scheeres, A. Rosengren, and J. W. McMahon, "The Dynamics of High Area-To-Mass Ratio Objects in Earth Orbit: The Effect of Solar Radiation Presssure," *21st Annual AAS/AIAA Spaceflight Mechanics Meeting*, New Orleans, Louisiana, February 13-17 2011.

[2] A. Rosengren and D. J. Scheeres, "Averaged Dynamics of HAMR Objects: Effects of Attitude and Earth Oblateness," *AAS/AIAA Astrodynamics Specialist Conference*, Girdwood, AK, July 31 - August 4 2011.

[3] B. A. Jones, G. H. Born, and G. Beylkin, "Comparisons of the Cubed-Sphere Gravity Model with the Spherical Harmonics," *Journal of Guidance, Control, and Dynamics*, Vol. 33, March-April 2010, pp. 415–425.

[4] B. A. Jones, G. H. Born, and G. Beylkin, "Sequential Orbit Determination with the Cubed-Sphere Gravity Model," *Journal of Spacecraft and Rockets*, Vol. 49, Jan.-Feb. 2012, pp. 145–156.

[5] R. P. Russell and N. Arora, "Global Point Mascon Models for Simple, Accurate, and Parallel Geopotential Computation," *21st Annual AAS/AIAA Spaceflight Mechanics Meeting*, New Orleans, Louisiana, February 13-17 2011.

[6] N. Arora and R. P. Russell, "Fast, Efficient and Adaptive Interpolation of the Geopotential," *AAS/AIAA Astrodynamics Specialist Conference*, Girdwood, AK, July 31 - August 4 2011.

[7] C. Runge, "Ueber die numerische Auflösung von Differentialgleichungen," *Mathematische Annalen*, Vol. 46, June 1895, pp. 167–178.

[8] W. M. Kutta, "Beitrag zur näherungsweisen Integration totaler Differentialgleichungen," *Zeitschrift für Mathematik und Physik*, Vol. 46, 1901, pp. 435–453.

[9] E. Fehlberg, "Classical Fifth-, Sixth-, Seventh-, and Eight-Order Runge-Kutta Formulas with Stepsize Control," Technical Report NASA-TR-R-287, NASA Marshall Space Flight Center, Huntsville, Alabama, October 1968.

[10] J. R. Dormand and R. J. Prince, "A family of embedded Runge-Kutta formulae," *Journal of Computational and Applied Mathematics*, Vol. 6, March 1980, pp. 19–26.

[11] R. J. Prince and J. R. Dormand, "High order embedded Runge-Kutta formulae," *Journal of Computational and Applied Mathematics*, Vol. 7, March 1981, pp. 67–75.

[12] J. Jackson, "Note on the Numerical Integration of $d^2x/dt^2 = f(x,t)$," *Monthly Notices of the Royal Astronomical Society*, Vol. 84, 1924, pp. 602–606.

[13] M. M. Berry and L. M. Healy, "Implementation of Gauss-Jackson Integration for Orbit Propagation," *Journal of Astronautical Sciences*, Vol. 52, July-September 2004, pp. 331–357.

[14] R. de Vogelaere, "Methods of Integration Which Preserve the Contact Transformation Property of the Hamiltonian Equations," Tech. Rep. 4, University of Notre Dame Department of Mathematics, 1956.

[15] R. D. Ruth, "A Canonical Integration Technique," *IEEE Transactions on Nuclear Science*, Vol. 30, August 1983, pp. 2669–2671.

[16] K. Feng, "On Difference Schemes and Symplectic Geometry," *Proceedings of the 5th International Symposium on Differential Geometry and Differential Equations*, Beijing, China, August 1984, pp. 42–48.

[17] J. Wisdom, "The Origin of the Kirkwood Gaps: A Mapping for Asteroidal Motion Near the 3/1 Commensurability," *The Astronomical Journal*, Vol. 87, March 1982, pp. 577–593.

[18] J. Wisdom, "Chaotic Behavior and the Origin of the 3/1 Kirkwood Gap," *Icarus*, Vol. 56, October 1983, pp. 51–74.

[19] J. Wisdom and M. Holman, "Symplectic Maps for the N-Body Problem," *Astronomical Journal*, Vol. 102, October 1991, pp. 1528–1538.

[20] E. Hairer, C. Lubich, and G. Wanner, *Geometric Numerical Integration : Structure-Preserving Algorithms for Ordinary Differential Equations*. No. 31 in Springer Series in Computational Mathematics, New York: Springer, 2002.

[21] V. I. Arnold, V. V. Kozlov, and A. I. Neishtadt, *Mathematical Aspects of Classical and Celestial Mechanics*, Vol. 3 of *Encyclopedia of Mathematical Sciences*. Springer, third ed., 2006.

[22] K. R. Meyer and G. R. Hall, *Introduction to Hamiltonian Dynamical Systems and the N-Body Problem*. New York: Springer-Verlag, 1992.

[23] B. Leimkuhler and S. Reich, *Simulating Hamiltonian Dynamics*, Vol. 1. New York: Cambridge University Press, 2004.

[24] A. Iserles, *A First Course in the Numerical Analysis of Differential Equations*. Cambridge University Press, second ed., 2009.

[25] B. L. Ehle, *On Padé Approximations to the Exponential Function and A-stable Methods for the Numerical Solution of Initial Value Problems*. Ph.d. thesis, University of Waterloo, Waterloo, ON, Canada, March 1969.

[26] J. C. Butcher, "A stability property of implicit Runge-Kutta methods," *BIT Numerical Mathematics*, Vol. 15, No. 4, 1975, pp. 358–361.

[27] P. W. Sharp, "Comparisons of integrators on a diverse collection of restricted three-body test problems," *IMA Journal of Numerical Analysis*, Vol. 24, No. 4, 2004, pp. 557–575.

[28] O. Montenbruck, "Numerical Integration Methods for Orbital Motion," *Celestial Mechanics and Dynamical Astronomy*, Vol. 53, 1992, pp. 59–69.

[29] K. Fox, "Numerical integration of the equations of motion in celestial mechanics," *Celestial Mechanics and Dynamical Astronomy*, Vol. 33, June 1984, pp. 127–142.

[30] T. E. Hull, W. H. Enright, B. M. Fellen, and A. E. Sedgwick, "Comparing Numerical Methods for Ordinary Differential Equations," *SIAM Journal on Numerical Analysis*, Vol. 9, December 1972, pp. 603–637.

[31] K. Burrage, *Parallel and Sequential Methods for Ordinary Differential Equations*. Oxford: Clarendon Press, 1995.

[32] L. F. Shampine and M. W. Reichelt, "The MATLAB ODE Suite," *SIAM Journal of Scientific Computing*, Vol. 18, January 1997, pp. 1–22.

[33] K. Hill and B. A. Jones, *TurboProp Version 4.0*. Colorado Center for Astrodynamics Research, May 2009.

[34] A. Iserles and S. P. Nørsett, "On the Theory of Parallel Runge-Kutta Methods," *IMA Journal of Numerical Analysis*, Vol. 10, No. 4, 1990, pp. 463–488.

[35] K. R. Jackson and S. P. Nørsett, "The Potential for Parallelism in Runge-Kutta Methods. Part 1: RK Formulas in Standard Form," *SIAM Journal on Numerical Analysis*, Vol. 32, February 1995, pp. 49–82.

[36] T. Eirola and J. M. Sanz-Serna, "Conservation of integrals and symplectic structure in the integration of differential equations by multistep methods," *Numerische Mathematik*, Vol. 61, No. 1, 1992, pp. 281–290.

[37] Y.-F. Tang, "The symplecticity of multi-step methods," *Computers and Mathematics with Applications*, Vol. 25, February 1993, pp. 83–90.

[38] Q.-D. Feng, Y.-D. Jiao, and Y.-F. Tang, "Conjugate symplecticity of second-order linear multi-step methods," *Journal of Computational and Applied Mathematics*, Vol. 203, June 2007, pp. 6–14.

[39] G. G. Dahlquist, "A Special Stability Problem for Linear Multistep Methods," *BIT Numerical Mathematics*, Vol. 3, No. 1, 1963, pp. 27–43.

[40] F. T. Krogh, "Predictor-Corrector Methods of High Order with Improved Stability Characteristics," *Journal of the ACM*, Vol. 13, July 1966, pp. 374–385.

[41] F. T. Krogh, "VODQ/SVDQ/DVDQ – Variable Order Integrators for the Numerical Solution of Ordinary Differential Equations," section 314 subroutine write-up, Jet Propulsion Laboratory, Pasadena, California, 1969.

[42] F. T. Krogh, "A Variable Step Variable Order Multistep Method for the Numerical Solution of Ordinary Differential Equations," *Information Processing 68: Proceedings of IFIP Congress 1968* (A. J. H. Morrell, ed.), Vol. 1 – Mathematics, Software, 1969, pp. 194–199.

[43] F. T. Krogh, "On Testing a Subroutine for the Numerical Integration of Ordinary Differential Equations," *Journal of the Association for Computing Machinery*, Vol. 1973, October 1973, pp. 545–562.

[44] F. T. Krogh, "Notes on a New Package for Ordinary Differential Equations," Computing Memorandum 361, California Institute of Technology, Jet Propulsion Laboratory, Section 914, Pasadena, California, May 8 1974.

[45] F. T. Krogh, "Variable Order Adams Method for Ordinary Differential Equations (DIVA)," tech. rep., Math à la Carte, http://mathalacarte.com/cb/mom.fcg/ya64, Tujunga, California, October 1975.

[46] S. Flanagan, T. Drain, T. Ely, and T. Martin-Mur, "Navigation and Missions Analysis Software for the Next Generation of JPL Missions," *16th International Symposium on Space Flight Dynamics*, Pasadena, California, 2001.

[47] T. D. Talbot and E. A. Rinderle, "Choice of Integrators for Use with a Variation-of-Parameters Formulation," *Deep Space Network Progress Report*, Vol. 1, November 1970, pp. 117–121.

[48] K. A. Papp, K. A. Innanen, and A. T. Patrick, "A Comparison of Five Algorithms for Numerical Computation in Galaxy Models," *Celestial Mechanics and Dynamical Astronomy*, Vol. 18, No. 3, 1978, pp. 277–286.

[49] L. F. Shampine and M. K. Gordon, *Computer Solution of Ordinary Differential Equations*. San Francisco: W. H. Freeman and Company, 1975.

[50] K. Wright, "Some relationships between implicit Runge-Kutta, collocation and Lanczos τ methods, and their stability properties," *BIT Numerical Mathematics*, Vol. 10, No. 2, 1970, pp. 217–227.

[51] P. C. Hammer and J. W. Hollingsworth, "Trapezoidal Methods of Approximating Solutions of Differential Equations," *Mathematical Tables and Other Aids to Computation*, Vol. 9, No. 51, 1955, pp. 92–96.

[52] J. C. Butcher, "Implicit Runge-Kutta Processes," *Mathematics of Computation*, Vol. 18, January 1964, pp. 50–64.

[53] B. L. Ehle, "High Order A-Stable Methods for the Numerical Solution of Systems of D.E.'s," *BIT Numerical Mathematics*, Vol. 8, No. 4, 1968, pp. 276–278.

[54] J. M. Sanz-Serna, "Runge-Kutta schemes for Hamiltonian Systems," *BIT Numerical Mathematics*, Vol. 28, No. 4, 1988, pp. 877–883.

[55] E. Hairer, G. Wanner, and S. P. Nørsett, *Solving Ordinary Differential Equations II: Stiff and Differential-Algebraic Problems*. Berlin Heidelberg New York: Springer-Verlag, second revised ed., 1993.

[56] J. M. Sanz-Serna and M. P. Calvo, *Numerical Hamiltonian Problems*. London, UK: Chapman and Hall, 1994.

[57] J. C. Butcher, *Numerical Methods for Ordinary Differential Equations*. Chichester, England: John Wiley and Sons, Ltd., second ed., 2008.

[58] A. L. Herman and B. A. Conway, "Direct Optimization Using Collocation Based on High-Order Gauss-Lobatto Rules," *Journal of Guidance, Control, and Dynamics*, Vol. 19, May-June 1996, pp. 592–599.

[59] A. L. Herman and B. A. Conway, "Optimal, Low-Thrust, Earth-Moon Orbit Transfer," *Journal of Guidance, Control, and Dynamics*, Vol. 21, January-February 1998, pp. 141–147.

[60] M. T. Ozimek, D. J. Grebow, and K. C. Howell, "Solar Sails and Lunar South Pole Coverage," *AIAA/AAS Astrodynamics Specialist Conference*, Honolulu, Hawaii, August 18-21 2008.

[61] M. T. Ozimek, D. J. Grebow, and K. C. Howell, "A Collocation Approach for Computing Solar Sail Lunar Pole-Sitter Orbits," *AIAA/AAS Astrodynamics Specialist Conference*, Pittsburgh, PA, August 9-13 2009.

[62] D. J. Grebow, M. T. Ozimek, and K. C. Howell, "Design of Optimal Low-Thrust Lunar Pole-Sitter Missions," *19th Annual AAS/AIAA Spaceflight Mechanics Meeting*, Savannah, Georgia, February 8-12 2009.

[63] D. J. Grebow, M. T. Ozimek, and K. C. Howell, "Advanced modeling of optimal low-thrust lunar pole-sitter trajectories," *Acta Astronautica*, Vol. 67, October-November 2010, pp. 991–1001.

[64] R. Barrio, M. Palacios, and A. Elipe, "Chebyshev Collocation Methods for Fast Orbit Determination," *Applied Mathematics and Computation*, Vol. 99, 1999, pp. 195–207.

[65] G. Beutler, *Methods of Celestial Mechanics. I: Physical, Mathematical, and Numerical Principles*. Berlin Heidelberg New York: Springer-Verlag, 2005.

[66] X. Bai, *Modified Chebyshev-Picard Iteration Methods for Solution of Initial Value Problems and Boundary Value Problems*. Ph.d. thesis, Texas A&M University, August 2010.

[67] B. K. Bradley, B. A. Jones, G. Beylkin, and P. Axelrad, "A New Numerical Integration Technique in Astrodynamics," *22nd Annual AAS/AIAA Spaceflight Mechanics Meeting*, (to be presented), Charleston, SC, Jan. 29 - Feb. 2 2012.

[68] P. J. van der Houwen and D. P. Sommeijer, "Parallel iteration of high-order Runge-Kutta methods with stepsize contol," *Journal of Computational and Applied Mathematics*, Vol. 29, 10 January 1990, pp. 111–127.

[69] M. P. Calvo, M. A. López-Marcos, and J. M. Sanz-Serna, "Variable step implementation of geometric integrators," *Applied Numerical Mathematics*, Vol. 28, September 1998, pp. 1–16.

[70] M. P. Laburta, "Starting Algorithms for IRK Methods," *Journal of Computational and Applied Mathematics*, Vol. 83, October 7 1997, pp. 269–288.

[71] M. P. Calvo, "High order starting iterates for implicit Runge-Kutta methods: an improvement for variable-step symplectic integerators," *IMA Journal of Numerical Analysis*, Vol. 22, No. 1, 2002, pp. 153–166.

[72] M. P. Calvo, M. P. Laburta, and J. I. Montijano, "Two-step high order starting values for implicit Runge-Kutta methods," *Advances in Computational Mathematics*, Vol. 19, No. 4, 2003, pp. 401–412.

[73] M. P. Calvo, M. P. Laburta, and J. I. Montijano, "Starting Algorithms for Gauss Runge-Kutta Methods for Hamiltonian Systems," *Computers and Mathematics with Applications*, Vol. 45, No. 1-3, 2003, pp. 401–410.

[74] M. P. Laburta, "Construction of Starting Algorithms for the RK-Gauss Methods," *Journal of Computational and Applied Mathematics*, Vol. 90, April 17 1998, pp. 239–261.

[75] H. Yoshida, "Recent Progress in the Theory and Application of Symplectic Integrators," *Celestial Mechanics and Dynamical Astronomy*, Vol. 56, March 1993, pp. 27–43.

[76] L. Kong, R. Liu, and X. Zheng, "A Survey on Symplectic and Multi-Symplectic Algorithms," *Applied Mathematics and Computation*, Vol. 186, March 2007, pp. 670–684.

[77] J. M. Sanz-Serna, "Symplectic Integrators for Hamiltonian Problems: An Overview," *Acta Numerica*, Vol. 1, 1991, pp. 243–286.

[78] D. Donnelly and E. Rogers, "Symplectic integrators: An introduction," *American Journal of Physics*, Vol. 73, October 2005, pp. 938–945.

[79] R and C. Scovel, "Equivariant Constrainted Symplectic Integration," *Journal of Nonlinear Science*, Vol. 5, No. 3, 1995, pp. 233–256.

[80] S. Reich, "Momentum conserving symplectic integrators," *Physica D: Nonlinear Phenomena*, Vol. 76, 15 September 1994, pp. 375–383.

[81] J. Touma and J. Wisdom, "Lie-Poisson integrators for rigid body dynamics in the solar system," *The Astronomical Journal*, Vol. 107, March 1994, pp. 1189–1202.

[82] G. J. Sussman and J. Wisdom, "Chaotic Evolution of the Solar System," *Science*, Vol. 257, July 1992, pp. 56–62.

[83] M. J. Duncan, H. F. Levinson, and S. M. Budd, "The Dynamical Structure of the Kuiper Belt," *The Astronomical Journal*, Vol. 110, December 1995, pp. 3073–3189.

[84] H. F. Levinson and M. J. Duncan, "The Long-Term Dynamical Behavior of Short-Period Comets," *Icarus*, Vol. 108, March 1994, pp. 18–36.

[85] H. Yoshida, "Construction of Higher Order Symplectic Integrators," *Physics Letters A*, Vol. 150, November 12 1990, pp. 262–268.

[86] P. Saha and S. Tremaine, "Symplectic Integrators for Solar System Dynamics," *Astronomical Journal*, Vol. 104, October 1992, pp. 1633–1640.

[87] H. Kinoshita, H. Yoshida, and H. Nakai, "Symplectic Integrators and Their Application to Dynamical Astronomy," *Celestial Mechanics and Dynamical Astronomy*, Vol. 50, No. 1, 1991, pp. 59–71.

[88] B. Gladman, M. Duncan, and J. Candy, "Symplectic Integrators for Long-Term Integrations in Celestial Mechanics," *Celestial Mechanics and Dynamical Astronomy*, Vol. 52, No. 3, 1991, pp. 221–240.

[89] R. A. Broucke, "A Comparison of the Symplectic and Other Numerical Integrators," *Annals of the New York Academy of Sciences*, Vol. 706, December 1993, pp. 126–147.

[90] M. J. Duncan, H. F. Levinson, and M. H. Lee, "A Multiple Time Step Symplectic Algorithm for Integrating Close Encounters," *The Astronomical Journal*, Vol. 116, October 1998, pp. 2067–2077.

[91] P. Saha and S. Tremaine, "Long-Term Planetary Integration with Individual Time Steps," *The Astronomical Journal*, Vol. 108, November 1994, pp. 1962–1969.

[92] M. P. Calvo and J. M. Sanz-Serna, "The Development of Variable-Step Symplectic Integrators, with Application to the Two-Body Problem," *SIAM Journal of Scientific Computing*, Vol. 14, July 1993, pp. 936–952.

[93] R. D. Skeel and C. W. Gear, "Does Variable Step Size Ruin a Symplectic Integrator?," *Physica D*, Vol. 60, November 1992, pp. 311–313.

[94] D. Stoffer, "Variables steps for reversible integration methods," *Computing*, Vol. 55, No. 1, 1995, pp. 1–22.

[95] P. Hut, J. Makino, and S. McMillan, "Building a better leapfrog," *The Astrophysical Journal*, Vol. 443, No. 2, 1995, pp. L93–L96.

[96] W. Huang and B. Leimkuhler, "The Adaptive Verlet Method," *SIAM Journal of Scientific Computing*, Vol. 18, No. 1, 1997, pp. 239–256.

[97] S. Mikkola, "Practical Symplectic Methods with Time Transformation for the Few-Body Problem," *Celestial Mechanics and Dynamical Astronomy*, Vol. 67, February 1997, pp. 145–165.

[98] S. Mikkola and P. Wiegert, "Regularizing Time Transformations in Symplectic and Composite Integration," *Celestial Mechanics and Dynamical Astronomy*, Vol. 82, No. 4, 2002, pp. 375–390.

[99] E. Hairer, "Variable time step integration with symplectic methods," *Applied Numerical Mathematics*, Vol. 25, November 1997, pp. 219–227.

[100] S. Reich, "Backward Error Analysis for Numerical Integrators," *SIAM Journal on Numerical Analysis*, Vol. 36, No. 5, 1999, pp. 1549–1570.

[101] S. Mikkola, "Efficient Symplectic Integration of Satellite Orbits," *Celestial Mechanics and Dynamical Astronomy*, Vol. 74, August 1999, pp. 275–285.

[102] S. Mikkola, "Non-Canonical Perturbations in Symplectic Integration," *Celestial Mechanics and Dynamical Astronomy*, Vol. 68, No. 3, 1998, pp. 249–255.

[103] R. Malhotra, "A Mapping Method for the Gravitational Few-Body Problem with Dissipation," *Celestial Mechanics and Dynamical Astronomy*, Vol. 60, No. 3, 1994, pp. 373–385.

[104] R. R. Cordeiro, R. S. Gomes, and R. V. Martins, "A mapping for nonconservative systems," *Celestial Mechanics and Dynamical Astronomy*, Vol. 65, No. 4, 1996, pp. 407–419.

[105] S. Breiter and G. Métris, "Symplectic Mapping for Satellites and Space Debris Including Nongravitational Forces," *Celestial Mechanics and Dynamical Astronomy*, Vol. 71, No. 2, 1999, pp. 79–94.

[106] S. Mikkola, P. L. Palmer, and Y. Hashida, "A Symplectic Orbital Estimator for Direct Tracking on Satellites," *The Journal of the Astronautical Sciences*, Vol. 48, January-March 2000, pp. 109–125.

[107] J. Anton, S. Trilles, and P. Mercier, "Study of Integration Schemes Suited for the Long-Term Extrapolation," *22nd International Symposium on Space Flight Dynamics*, São José dos Campos, SP, Brazil, Feb. 28 - Mar. 5 2011.

[108] R. I. McLachlan and G. R. W. Quispel, "Splitting methods," *Acta Numerica*, Vol. 11, 2002, pp. 341–434.

[109] W. Kahan and R.-C. Li, "Composition Constants for Raising the Orders of Unconventional Schemes for Ordinary Differential Equations," *Mathematics of Computation*, Vol. 66, No. 219, 1997, pp. 1089–1099.

[110] W. Kahan, "Further remarks on reducing truncation errors," *Communications of the ACM*, Vol. 8, January 1965, p. 40.

[111] O. Møller, "Quasi Double-Precision in Floating Point Addition," *BIT Numerical Mathematics*, Vol. 5, No. 1, 1965, pp. 37–50.

[112] B. Tapley, J. Ries, S. Bettadpur, D. Chambers, M. Cheng, F. Condi, B. Gunter, Z. Kang, P. Nagel, R. Pastor, T. Pekker, S. Poole, and F. Wang, "GGM02 - An Improved Earth Gravity Field Model from GRACE," *Journal of Geodesy*, Vol. 79, No. 8, 2005, pp. 467–478.

[113] D. A. Vallado and W. D. McClain, *Fundamentals of Astrodynamics and Applications*. Hawthorne, CA and New York, NY: Microcosm Press and Springer, third ed., 2007.

[114] Nautical Almanac Office, *The Astronomical Almanac For the Year 2006*. United States Naval Observatory, Washington, DC, 2004.

[115] M. Preto and S. Tremaine, "A Class of Symplectic Integrators with Adaptive Time Step for Separable Hamiltonian Systems," *Astronomical Journal*, Vol. 118, November 1999, pp. 2532–2541.